Electronic Supplementary Material (ESI) for New Journal of Chemistry.

Interaction of Caffeic Acid with Bovine Serum Albumin is Complex: Calorimetric, Spectroscopic and Molecular Docking Evidence

Aurica Precupas, Romica Sandu, Anca Ruxandra Leontieş, Dan-Florin Anghel, Vlad Tudor Popa[*]

"Ilie Murgulescu" Institute of Physical Chemistry of the Romanian Academy, Splaiul Independentei 202, Bucharest, 060021, Romania.

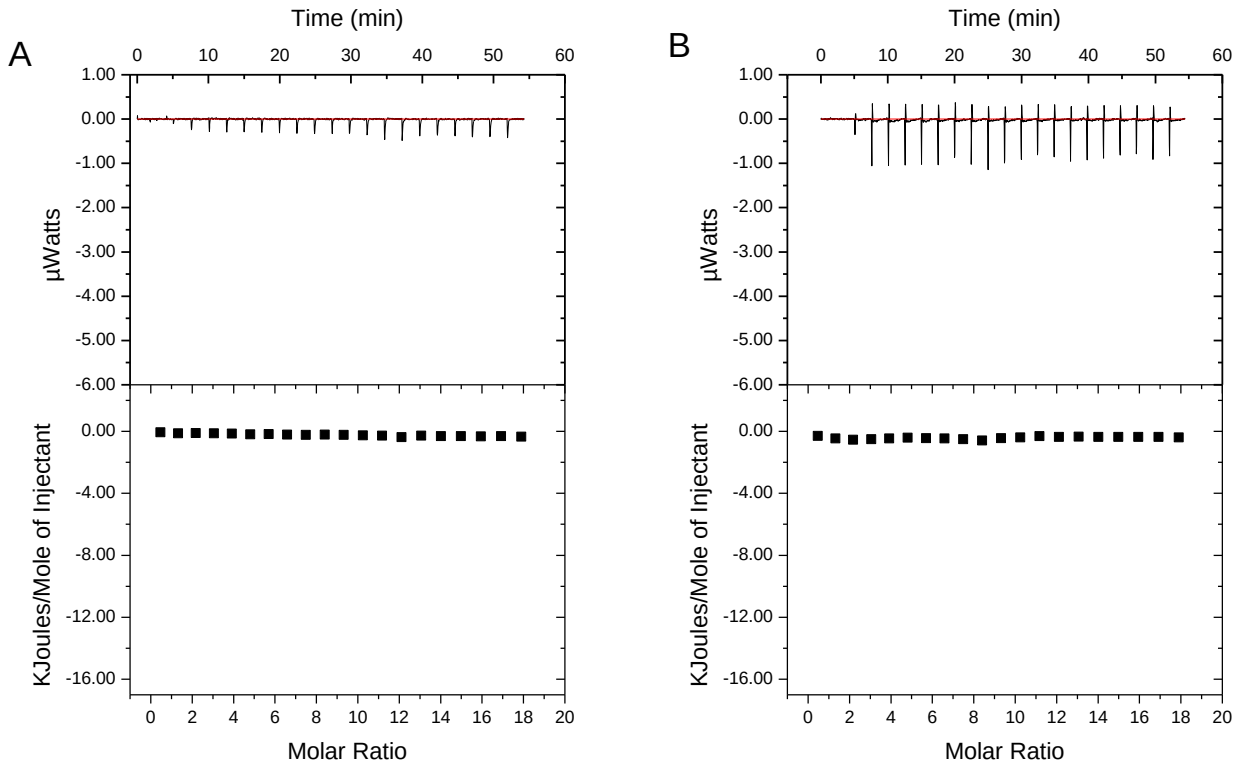

Fig. S1 ITC binding isotherm displaying the raw data for dilution effect for (A) BSA and (B) CA at 298 K in 0.1 M phosphate buffer (pH 7.4).

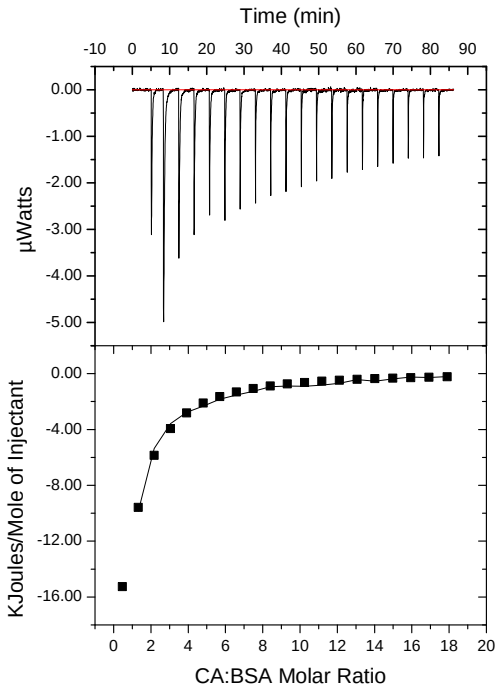

Model: OneSites

Reduced $\chi^2 = 3121$

$N = 9.61\times10^{-6} \pm 0.611$ Sites

$K = 8.73\times10^{3} \pm 1.62\times10^{3}\ M^{-1}$

$\Delta H = -4.376\times10^{9} \pm 2.779\times10^{14}\ J\ mol^{-1}$

$\Delta S = -1.47\times10^{7}\ J\ mol^{-1}\ K^{-1}$

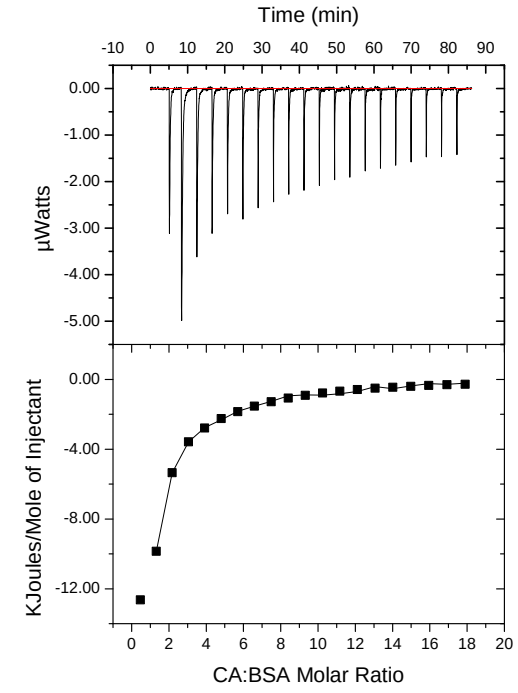

Model: TwoSites

Reduced $\chi^2 = 471.5$

$N_1 = 1.16 \pm 0.528$ Sites

$K_1 = 2.99\times10^{5} \pm 6.10\times10^{5}\ M^{-1}$

$\Delta H_1 = -1.40\times10^{4} \pm 1.01\times10^{4}\ J\ mol^{-1}$

$\Delta S_1 = 58.0\ J\ mol^{-1}\ K^{-1}$

$N_2 = 2.84 \pm 2.95$ Sites

$K_2 = 5.55\times10^{3} \pm 1.93\times10^{3}\ M^{-1}$

$\Delta H_2 = -9323 \pm 1.11\times10^{4}\ J\ mol^{-1}$

$\Delta S_2 = 40.4\ J\ mol^{-1}\ K^{-1}$

Fig. S2 ITC profile for BSA titration with CA. The solid line represents the non-linear least-squares fit to the experimental data points using OneSites Model/TwoSites Model.

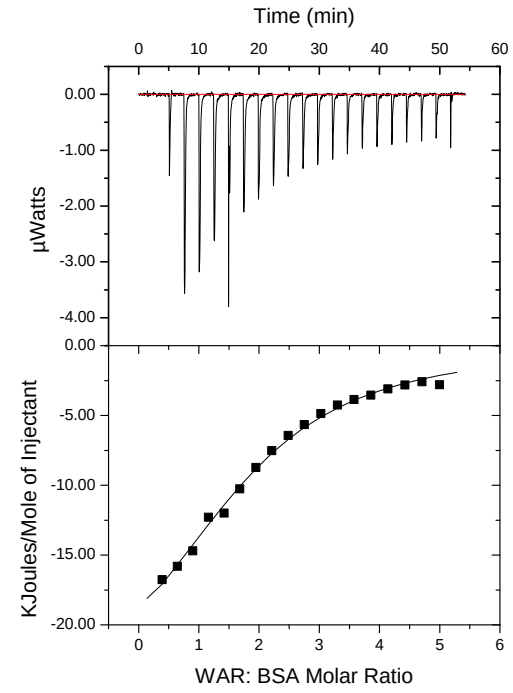

Model: OneSites

Reduced $\chi^2 = 6797$

$N = 1.81 \pm 0.096$ Sites

$K = 2.15\times10^4 \pm 2.59\times10^3\ M^{-1}$

$\Delta H = -2.79\times10^4 \pm 2.08\times10^3\ J\ mol^{-1}$

$\Delta S = -10.70\ J\ mol^{-1}\ K^{-1}$

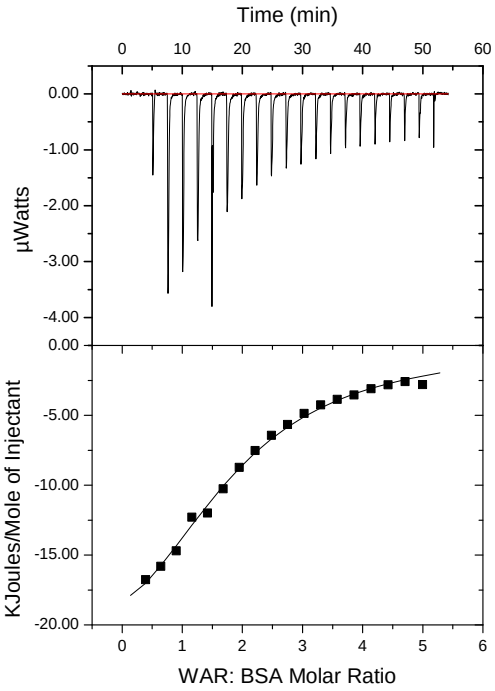

Model: Two Sites sequential binding

Reduced $\chi^2 = 6239$

$K_1 = 6.66\times10^4 \pm 5.4\times10^3\ M^{-1}$

$\Delta H_1 = -2.362\times10^4 \pm 0.69\times10^3\ J\ mol^{-1}$

$\Delta S_1 = 13.1\ J\ mol^{-1}\ K^{-1}$

$K_2 = 1.03\times10^4 \pm 0.98\times10^3\ M^{-1}$

$\Delta H_2 = -2.785\times10^4 \pm 1.53\times10^3\ J\ mol^{-1}$

$\Delta S_2 = -16.6\ J\ mol^{-1}\ K^{-1}$

Fig. S3 A representative ITC profile displaying the raw data for the integrated heat change (after appropriate correction for heat of dilution) for WAR (1.5×10^{-3} M) with BSA (5×10^{-5} M) interaction at 298 K in 0.1 M phosphate buffer pH 7.4. The solid line represents the non-linear least-squares fit to the experimental data points using OneSites Model/Two Sites sequential binding Model.

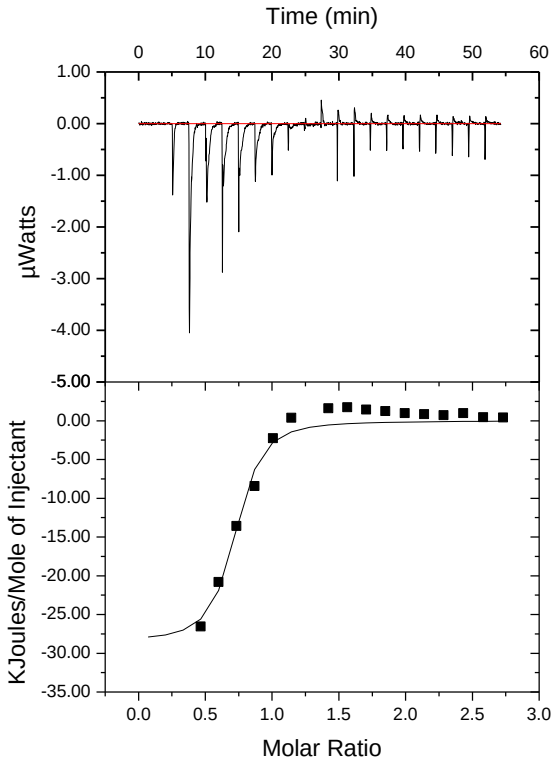

Model: OneSites

Reduced χ^2 = 1.289E5

N = 0.68 ± 0.028 Sites

K = 1.44×10^6 ± 0.69×10^6 M^{-1}

$\Delta H = -2.85\times10^4 \pm 2.56\times10^3$ J mol^{-1}

ΔS = 22.30 J mol^{-1} K^{-1}

Fig. S4 A representative ITC profile displaying the raw data for the integrated heat change (after appropriate correction for heat of dilution) for BSA (5×10^{-5} M) with IBP (7.75×10^{-4} M) interaction at 298 K in 0.1 M phosphate buffer pH 7.4.

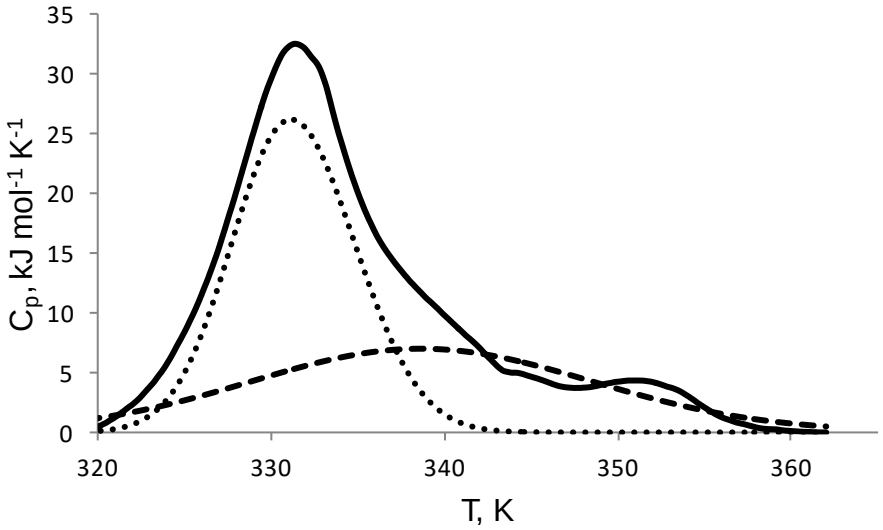

Fig. S5. PeakFit decomposition of DSC thermogram for BSA thermal denaturation. Albumin concentration is 1.05×10^{-4} M, scan rate of 1 K/min. The raw data is represented by solid line, PeakFit component 1 by dotted line and PeakFit component 2 by dashed line.

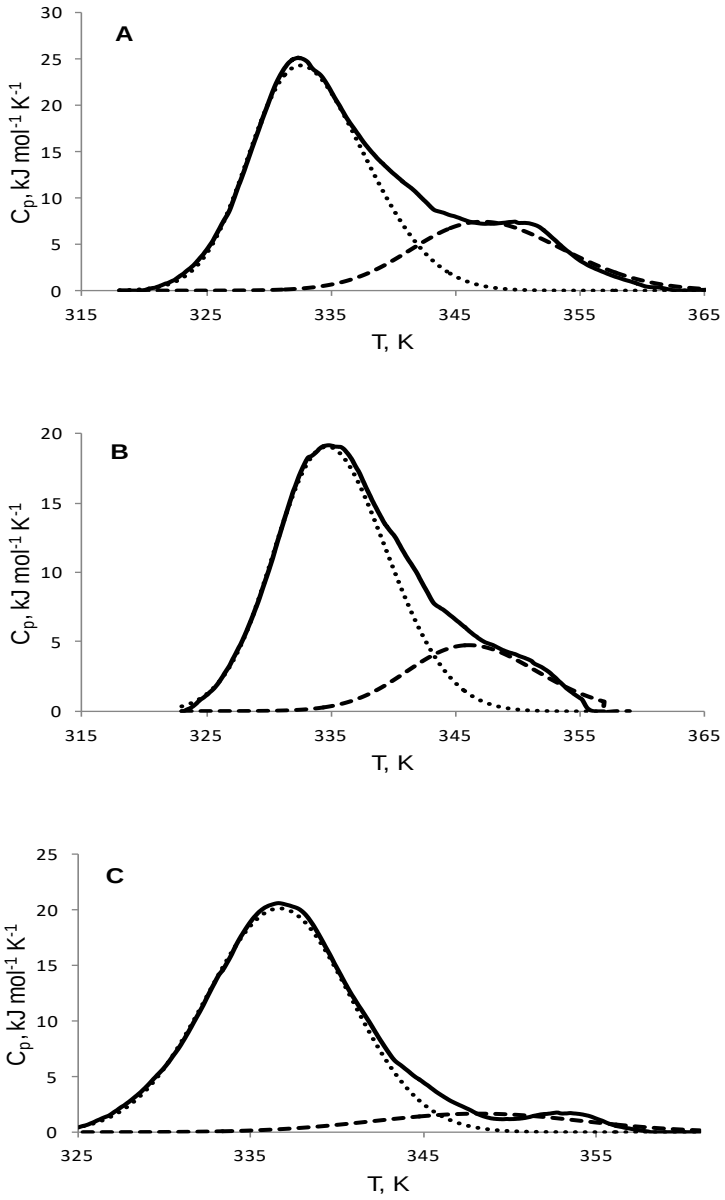

Fig. S6 PeakFit decomposition of DSC thermogram of CA: BSA thermal denaturation at different molar ratio (A) 1:1, (B) 3.5:1, (C) 20:1. Albumin concentration is 1.05×10^{-4} M, scan rate of 1 K/min. The raw data is represented by solid line, PeakFit component 1 by dotted line and PeakFit component 2 by dashed line.

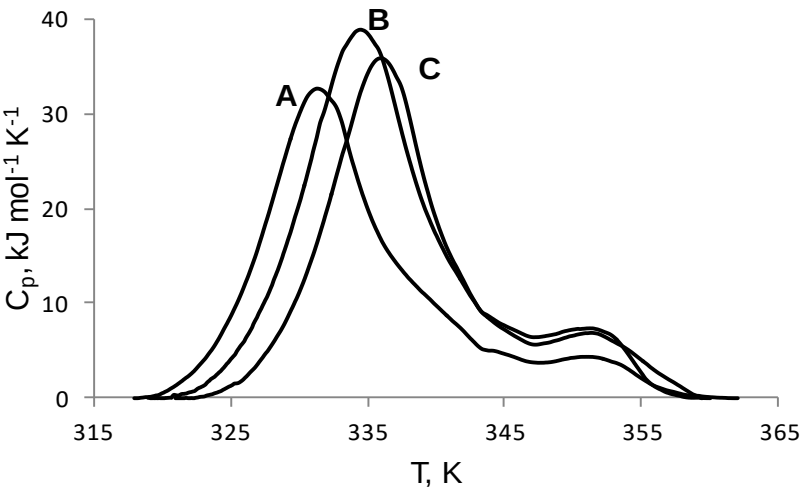

Fig. S7 Influence of different concentrations of WAR on BSA thermal denaturation: (A) WAR: BSA 0, (B) WAR: BSA 1:1, (C) WAR: BSA 3:1 molar ratios.

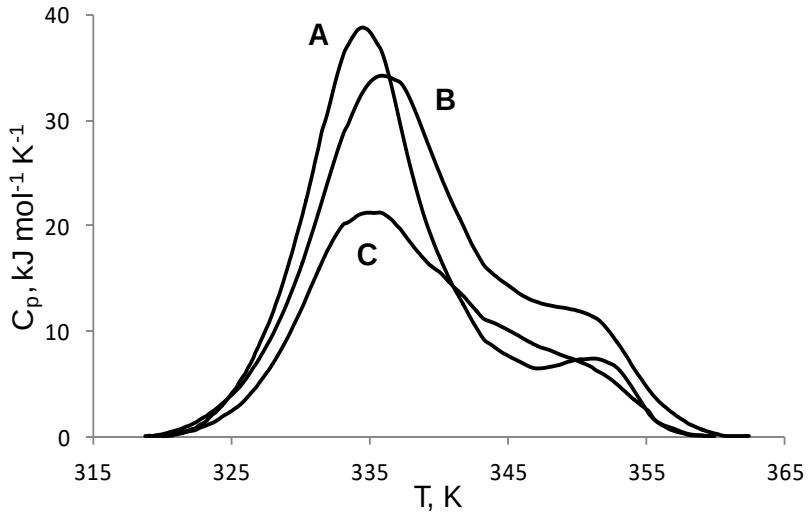

Fig. S8 Influence of competitive binding of WAR and CA on BSA thermal denaturation: (A) WAR: BSA 1:1, (B) WAR: BSA 1:1 and CA 3.70×10^{-4} M, (C) BSA and CA 3.70×10^{-4} M.

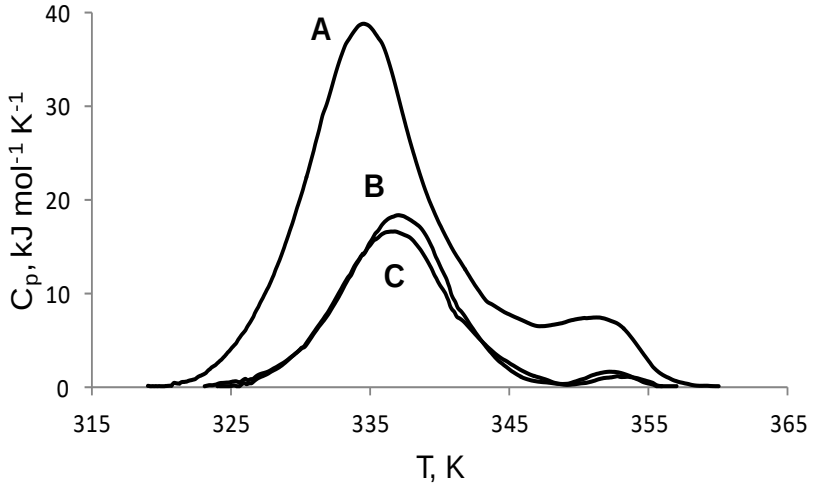

Fig. S9 Influence of competitive binding of WAR and CA on BSA thermal denaturation: (A) WAR: BSA 1:1, (B) WAR: BSA 1:1 and CA 2.10×10^{-3} M, (C) BSA and CA 2.10×10^{-3} M.

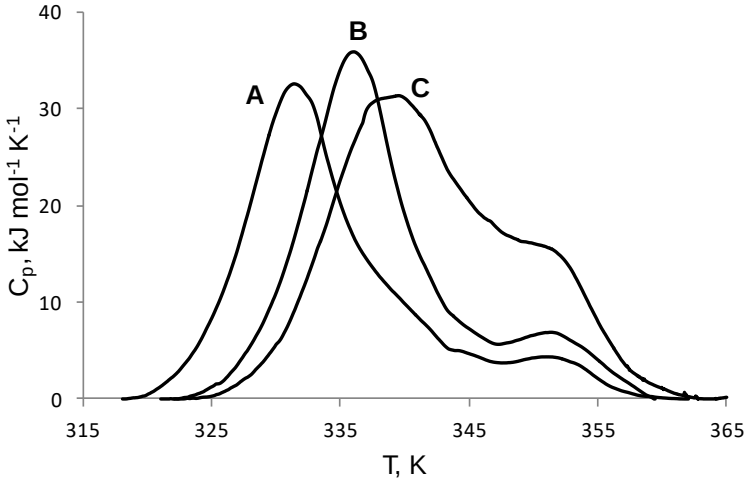

Fig. S10 Influence of competitive binding of WAR and CA on BSA thermal denaturation: (A) BSA, (B) WAR: BSA 3:1, (C) WAR: BSA 3:1 and CA 3.70×10^{-4} M.

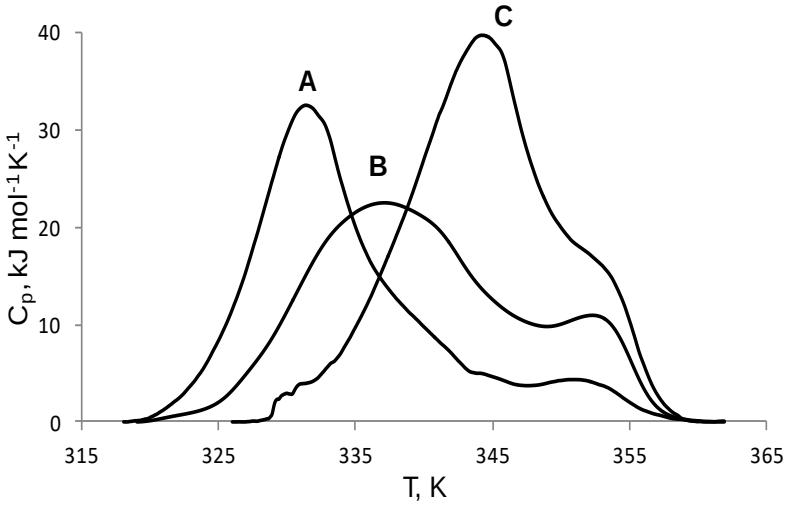

Fig. S11 Influence of different concentrations of IBP on BSA thermal denaturation: (A) IBP: BSA 0, (B) IBP: BSA 1:1, (C) IBP: BSA 3:1 molar ratio.

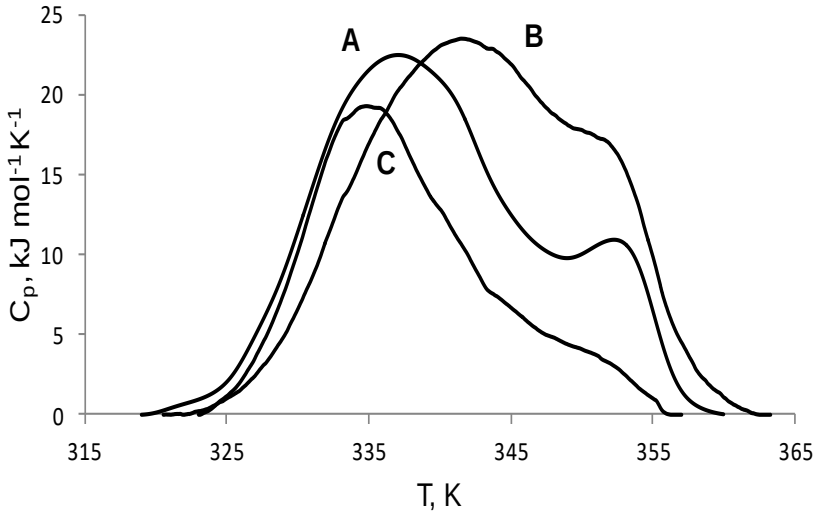

Fig. S12 Influence of competitive binding of IBP and CA on BSA thermal denaturation: (A) IBP: BSA 1:1, (B) IBP: BSA 1:1 and CA 3.70×10^{-4} M, (C) BSA and CA 3.70×10^{-4} M.

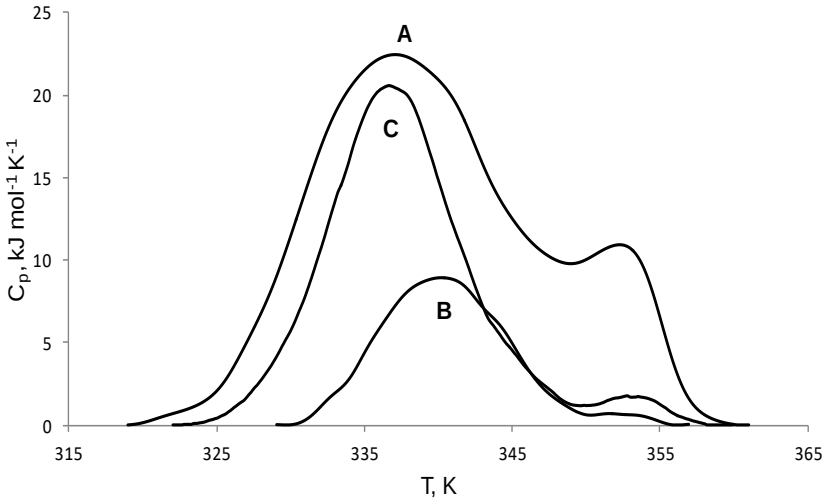

Fig. S13 Influence of competitive binding of IBP and CA on BSA thermal denaturation: (A) IBP: BSA 1:1, (B) IBP: BSA 1:1 and CA 2.10×10^{-3} M, (C) BSA and CA 2.10×10^{-3} M.

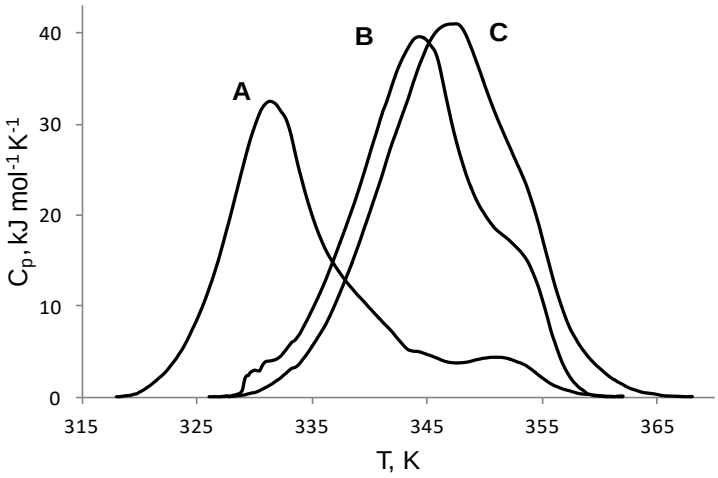

Fig. S14 Influence of competitive binding of IBP and CA on BSA thermal denaturation: (A) IBP: BSA 0, (B) IBP: BSA 3:1, (C) IBP: BSA 3:1 and CA 3.70×10^{-4} M.

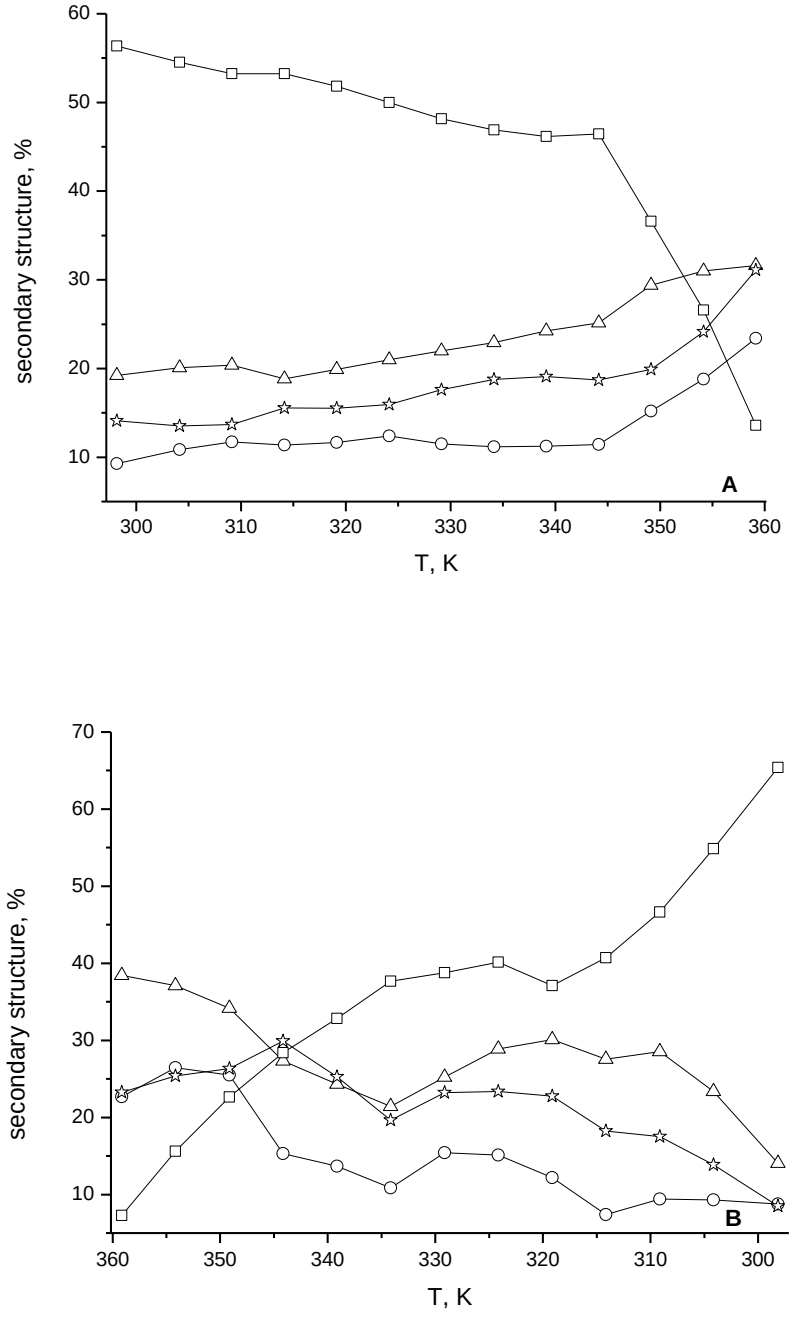

Fig. S15 Temperature variation of the **s**econdary structure content (determined on Dichroweb) for BSA (squares- α-helix, triangles-β-sheets, circles- turns, star-unordered, A-unfolding, B-refolding).

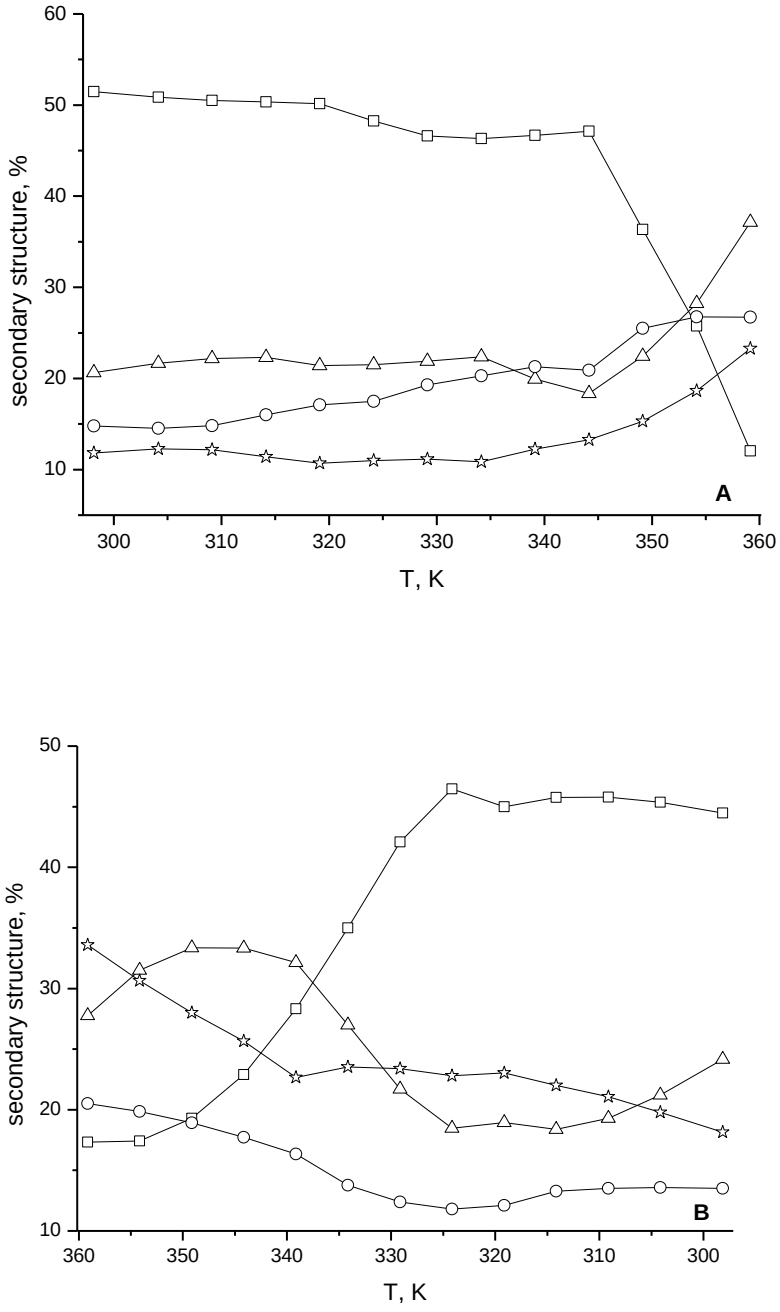

Fig. S16 Temperature variation of the **s**econdary structure content (determined on Dichroweb) for CA: BSA = 1:1 molar ratio (squares- α-helix, triangles-β-sheets, circles- turns, star-unordered, A-unfolding, B-refolding).

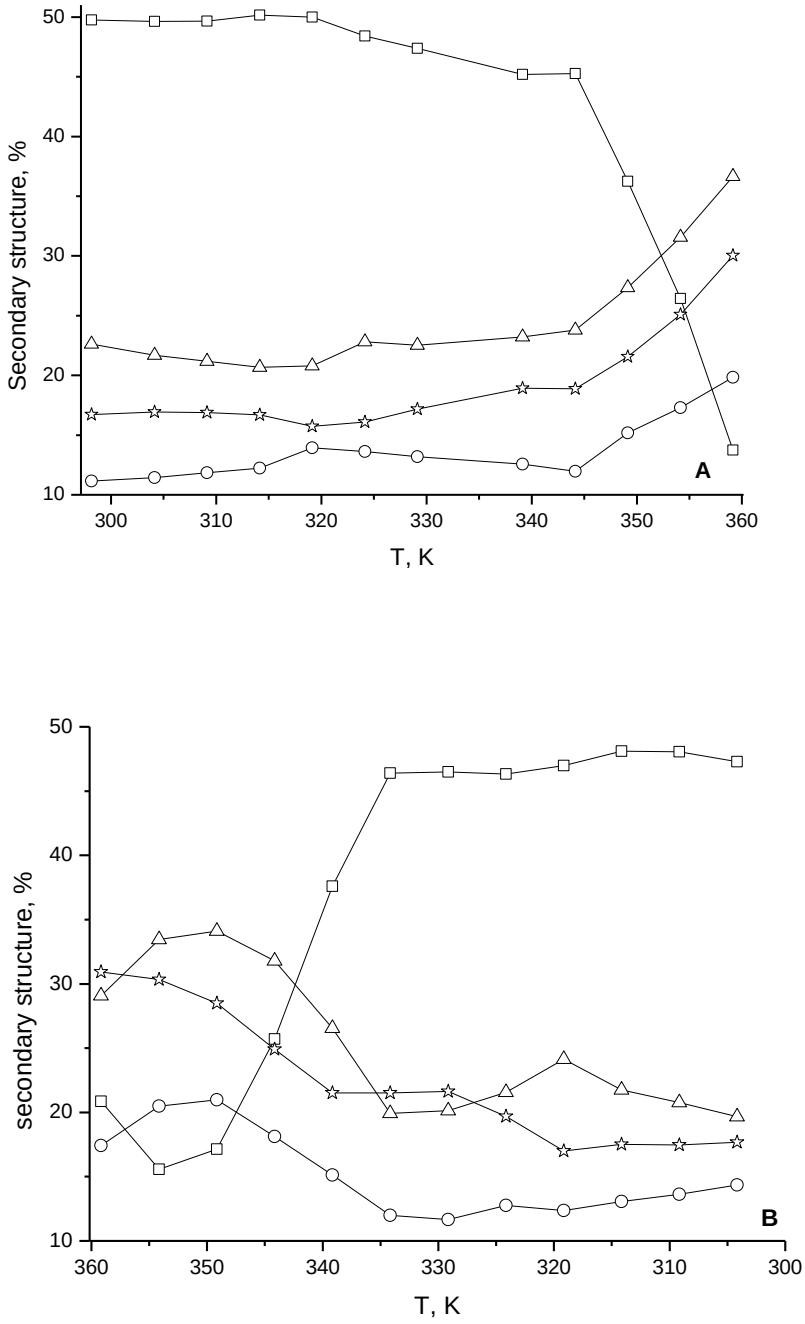

Fig. S17 Temperature variation of the **s**econdary structure content (determined on Dichroweb) for CA: BSA = 20:1 molar ratio (squares- α-helix, triangles-β-sheets, circles- turns, star- unordered, A-unfolding, B-refolding).